Bioorganic Chemistry 90 (2019) 103032

Contents lists available at ScienceDirect

Bioorganic Chemistry

journal homepage: www.elsevier.com/locate/bioorg

Novel cytisine derivatives exert anti-liver fibrosis effect via PI3K/Akt/Smad pathway

Sheng Tang[1], Yinghong Li[1], Yunyang Bao, Zhiting Dai, Tianyu Niu, Kun Wang, Hongwei He**, Danqing Song*

Institute of Medicinal Biotechnology, Peking Union Medical College and Chinese Academy of Medical Sciences, Beijing 100050, China

ARTICLE INFO

Keywords:
Liver fibrosis
Cytisine
Structure-activity relationship
Fibrogenetic protein
COL1A1

ABSTRACT

A series of new cytisine derivatives with a unique endocyclic scaffold were synthesized and evaluated for their inhibitory effect on collagen α1 (I) (COL1A1) promotor in human LX2 cells, taking cytisine as the lead. Structure-activity relationship (SAR) revealed that introducing a 12*N*-benzyl substitution might significantly enhance the activity. Compound **5f** exhibited a promising inhibitory potency against COL1A1 with an IC_{50} value of 12.8 μM in human LX2 cells, and an inspiring inhibition activity against COL1A1 on both mRNA and protein levels. It also effectively inhibited the expression of α smooth muscle actin (α-SMA), connective tissue growth factor (CTGA), matrix metalloprotein 2 (MMP-2), and transforming growth factor β1 (TGFβ1), indicating an extensive inhibitory effect against fibrogenetic proteins. In addition, compound **5f** displayed reasonable PK and safety profiles. The primary mechanism study indicated that it might repress the hepatic fibrogenesis via PI3K/Akt/Smad signaling pathway. The results provided powerful information for further structure optimization, and compound **5f** was selected as a novel anti-liver fibrosis agent for further investigation.

1. Introduction

Liver fibrosis is a histological hallmark of liver injury, and persistent liver fibrosis leads to cirrhosis, hepatoma, and liver failure [1]. A variety of pathogens and factors can trigger liver fibrogenesis, including cholestasis, hepatic viral infection and nonalcoholic steatohepatitis (NASH) as well as drug toxicity [2,3]. In the last decades, an immense effort has been undertaken to elucidate the mechanisms of liver fibrosis and to develop therapeutic approaches. Although a large number of candidates displayed antifibrotic properties *in vivo*, none of them has yet been approved for clinical use [4–6]. Up to date, there is still no effective therapy available for the treatment of liver fibrosis [7], thus, identifying and searching for an effective antifibrotic therapy is a major unmet clinical need [1].

Liver fibrosis is characterized by the excessive deposition of extracellular matrix (ECM) proteins [8]. Under persistent liver damage, hepatic stellate cells (HSCs) are continuously activated and converted into myofibroblasts, which are the major source of ECM and the principal cell type involved in liver fibrogenesis [9,10]. Transforming growth factor β1 (TGFβ1) is closely related to liver fibrosis, and considered as one of the most important fibrotic cytokines known so far [11]. In response to fibrogenic stimuli, such as an increased level of TGFβ1, HSCs activate into myofibroblasts and migrate to the site of injury, where they express fibrogenic genes such as collagen α1 (I) (COL1A1) and α smooth muscle actin (α-SMA) [12]. Based on the fact that the expression of COL1A1 promotor is elevated by TGFβ1, a luciferase screening cell model based on COL1A1 promoter was established earlier in our group [13], and was successfully applied to the screening and evaluation of anti-hepatic fibrosis drug candidates [14,15]. The *in vivo* pharmacodynamics study confirmed that compounds down-regulating the expression of COL1A1 promoter could effectively reverse liver fibrosis *in vivo* [15].

In our continuous effort to discover innovative compounds against liver fibrosis, our Chinese natural product library was screened, using the COL1A1 promotor-based screening cell model mentioned above in human hepatic stellate LX-2 cells [13]. Cytisine (Fig. 1), a major active constituent of *Laburnum anagyroides* [16] that had been used in clinic to deal with the treatment of nicotine addiction [17] and also showed a wide range of biological activities, such as analgesic, antihypertensive, inotropic, antispasmodic, antioxidant, and insecticidal activities [16],

* Corresponding author.
** Corresponding author.
E-mail addresses: hehwei@imb.pumc.edu.cn (H. He), songdanqingsdq@imb.pumc.edu.cn (D. Song).
[1] These authors made equal contributions to the work.

https://doi.org/10.1016/j.bioorg.2019.103032
Received 2 April 2019; Received in revised form 20 May 2019; Accepted 3 June 2019
Available online 08 June 2019

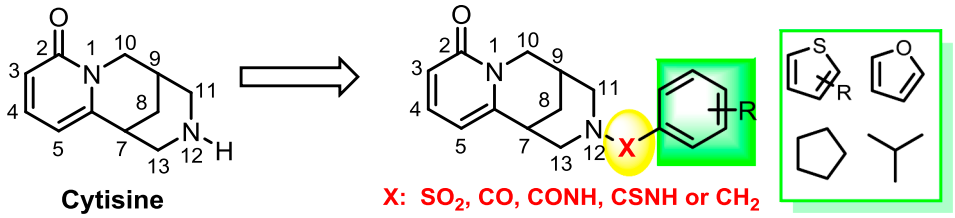

Fig. 1. The chemical structure of cytosine and modification strategy.

was identified as an anti-liver fibrosis hit. It displayed a mild effect against COL1A1 with an inhibitory rate of 9.53% at the concentration of 80 μM. Its unique endocyclic scaffold and specific biological activity greatly spurred us to further explore the structure–activity relationship (SAR) of its kind, in an effort to develop a new class of anti-hepatic fibrosis candidates.

As depicted in Fig. 1, various substituents were attached at the 12-position of cytisine, by which a series of novel 12*N*-substituted cytisine derivatives were designed, synthesized and evaluated for their activity on inhibiting COL1A1 promotor, taking cytisine as the lead. Furthermore, the effects of the key compounds on other fibrogenetic proteins in LX2 cells, such as α-SMA, connective tissue growth factor (CTGA) and matrix metalloprotein 2 (MMP-2) were also referred to. The metabolic stability and safety evaluation as well as primary mode of action of the key compounds were also carried out in the present study.

2. Result and discussion

2.1. Chemistry

A total of twenty-six new cytisine derivatives were prepared from commercially available cytisine with purity over 95% as the starting material, which was purchased from Xi'an Tianbao Biotechnology Co., Ltd. (Shanxi, China).

As described in Scheme 1, the target 12*N*-acyl cytisine products **1a–d** were gained via the reaction of cytisine and benzoyl or furan formyl chloride in an equimolar ratio in yields of 50–68%, using triethylamine as deacid reagent [16]. Similarly, the 12*N*-benzenesulfonyl cytisine derivatives **2a** and **2b** were obtained by *N*-sulfonylation of cytisine in CH_2Cl_2 with yields of 46% and 85% respectively. The 12*N*-benzeneanimo formyl products **3a–g** and 12*N*-benzeneanimo thioformyl products **4a** and **4b** were acquired by the reaction of cytisine and isocyanates or thioisocyanates in the presence of triethylamine in 32–78% yields. The preparations of 12*N*-benzyl products **5a–i** were similar to that of **1a–d,** in which different benzyl bromides were applied instead. Compound **5k** was achieved by the reaction of cytisine and dibenzyl chloride in a 40% yield. The hydrolysis of **5i** in 10% NaOH generated **5j** in a 76% yield. All the final products were purified by flash column chromatography on silica gel with CH_2Cl_2/CH_3OH as the eluent.

2.2. SAR for inhibition of COL1A1 promotor of the target compounds in LX-2 cells

A single luciferase reporter gene detection model was applied to screen the inhibitory effects towards COL1A1 promotor of all target compounds in LX-2 cells at the concentration of 80 μM, taking EGCG (25 μM) [18] and cytisine (80 μM) as the references. The LX2 cell lines were transfected with COL1A1 promotor luciferase plasmid pGL4.17-COL1A1P using lipofactamine 2000 followed the standard protocol

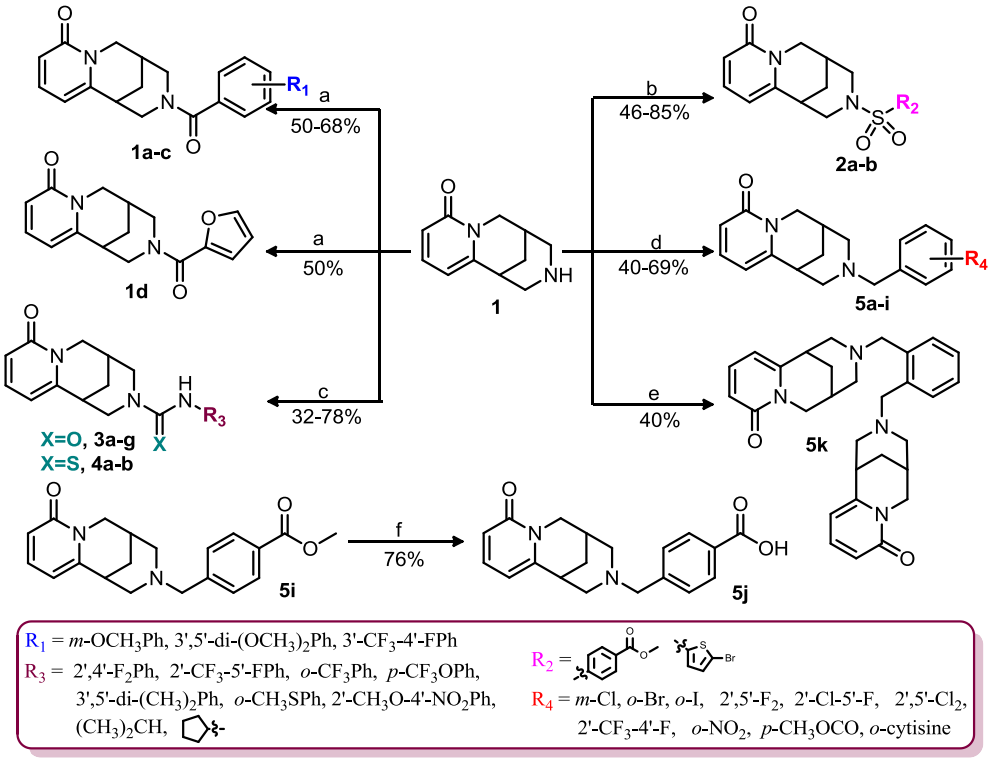

Scheme 1. (a) TEA, benzoyl chloride, CH_2Cl_2, r.t.; (b) TEA, benzenesulfonyl chloride, CH_2Cl_2, r.t.; (c) isocyanate, CH_2Cl_2, rt.; (d) TEA, benzyl bromide, CH_2Cl_2, r.t.; (e) TEA, 1,2-bis(chloromethyl)- benzene, CH_2Cl_2, r.t.; (f) 20% NaOH, 3 h, r.t.

Table 1
Inhibition on COL1A1 promotor of target compounds and cytotoxicity of key compounds.

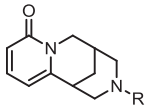
1a-d; 2a, 2b; 3a-g; 4a, 4b; 5a-j

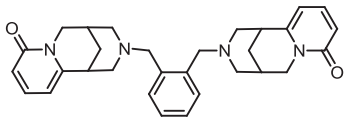
5k

Code	R	Inhibition rate[a](%)	Inhibition rate[b](%)	IC_{50} (μM)[c]	CC_{50} (μM)[d]	SI
Cytisine	/	9.53 ± 1.65	NT[e]	NT	NT	NT
1a	*m*-$CH_3OC_6H_4CO$	60.9 ± 11.6	41.1 ± 22.4	NT	NT	NT
1b	3′,5′-di-$CH_3OC_6H_3CO$	7.57 ± 12.5	NT	NT	NT	NT
1c	3′-CF_3-4′-FC_6H_3CO	8.29 ± 25.8	NT	NT	NT	NT
1d		4.43 ± 17.5	NT	NT	NT	NT
2a	*p*-$CH_3O_2CC_6H_4SO_2$	13.5 ± 30.9	NT	NT	NT	NT
2b		7.85 ± 14.8	NT	NT	NT	NT
3a	2′,4′-di-FC_6H_3NHCO	10.6 ± 19.5	NT	NT	NT	NT
3b	2′-CF_3-5′-FC_6H_3NHCO	25.6 ± 14.2	NT	NT	NT	NT
3c	*o*-$CF_3C_6H_4NHCO$	51.4 ± 8.32	42.8 ± 1.39	NT	NT	NT
3d	*p*-$CF_3OC_6H_4NHCO$	36.9 ± 21.2	NT	NT	NT	NT
3e	3′,5′-di-$CH_3C_6H_3NHCO$	39.2 ± 22.7	NT	NT	NT	NT
3f	$(CH_3)_2CHNHCO$	40.3 ± 19.7	NT	NT	NT	NT
3g		25.1 ± 14.4	NT	NT	NT	NT
4a	*o*-$CH_3SC_6H_4NHCS$	52.7 ± 10.2	30.2 ± 3.9	NT	NT	NT
4b	2′-CH_3O-4′-$NO_2C_6H_3NHCS$	11.9 ± 17.8	NT	NT	NT	NT
5a	*m*-$ClC_6H_4CH_2$	81.3 ± 9.14	62.7 ± 10.5	NT	NT	NT
5b	*o*-$BrC_6H_4CH_2$	96.1 ± 2.29	44.6 ± 16.5	NT	NT	NT
5c	o-$IC_6H_4CH_2$	94.0 ± 4.80	74.5 ± 6.08	22.2 ± 0.97	> 400	> 18.0
5d	2′,5′-di-$FC_6H_3CH_2$	55.9 ± 9.20	52.0 ± 5.49	NT	NT	NT
5e	2′-Cl-5′-$FC_6H_3CH_2$	87.8 ± 4.24	53.6 ± 25.4	NT	NT	NT
5f	2′,5′-di-$ClC_6H_3CH_2$	99.7 ± 0.12	86.4 ± 9.61	12.8 ± 3.14	> 400	> 32.3
5g	2′-CF_3-4′-$FC_6H_3CH_2$	98.1 ± 2.00	81.7 ± 3.67	16.9 ± 1.03	247 ± 24.3	14.6
5h	*o*-$NO_2C_6H_4CH_2$	38.5 ± 8.52	NT	NT	NT	NT
5i	*p*-$CH_3OCOC_6H_4CH_2$	48.1 ± 4.33	NT	NT	NT	NT
5j	*p*-$HO_2CC_6H_4CH_2$	43.8 ± 15.6	NT	NT	NT	NT
5k	/	47.6 ± 11.9	NT	NT	NT	NT
EGCG	/	27.5 ± 7.9[f]	NT	NT	NT	NT
DMSO	/	2.9 ± 0	2.9 ± 0	NT	NT	NT

[a] At the concentration of 80 μM.
[b] At the concentration of 40 μM.
[c] Concentration required to inhibit half maximal of COL1A1 promotor expression.
[d] Cytotoxic concentration required to inhibit HepG2 cells cell growth by 50%.
[e] Not tested.
[f] At the concentration of 25 μM.

(Invitrogen) for 24 h, then treated simultaneously with TGFβ1 and a tested compounds for 24 h [13]. The structures and inhibitory effects (%) of all target compounds were shown in Table 1.

The SAR analysis for anti-COL1A1 activity was mainly concentrated on the influence of different types of substituents on the 12-nitrogen atom, by which several series of new 12*N*-substituted cytisine derivatives, such as 12*N*-benzoyl (**1a–c**), 12*N*-furanformyl (**1d**), 12*N*-sulfonyl (**2a** and **2b**), 12*N*-aminoacyl (**3a–g**), 12*N*-benzenaminothioacyl (**4a** and **4b**) and 12*N*-benzyl (**5a–k**), were generated and evaluated. As described in Table 1, the introduction of a *m*-methyoxyl on the benzene ring (**1a**) caused a significant increase in activity with the inhibitory rate of 60.9% at the concentration of 80 μM, while di-substituted compounds **1b** and **1c** gave decreased inhibition effects compared with the lead. Then, benzoyl was replaced by its bioisostere 2-furanformyl, and the generated analogue **1d** showed an obvious decline in activity, indicating the advantage of benzene ring over furan in activity.

Next, the benzene ring was retained, and acyl linker was replaced with sulfonyl, and the generated benzenesulfonyl **2a** and thiofuransulfonyl analogue **2b** only gave comparable activities to cytisine, hinting that sulfonyl was not active. Then acyl group was replaced with aminoacyl to generate derivatives **3a–e**, and all of them enhanced activity to some extent. Furthermore, benzene ring was respectively replaced with isopropyl (**3f**) and cyclopentyl (**3g**), and the improved activity was also observed. Then, aminoacyl was replaced by its biostere aminothioacyl, and the generated analogues **4a** and **4b** gave enhanced or comparative activity as compared to cytisine. And the top compounds **3e** and **4a** in both series gave the comparable inhibitory rates of 51.4% and 52.7%, respectively.

At last, 12*N*-benzyl motif was introduced and the corresponding target derivatives **5a–k** displayed significantly improved activities compared with cytisine. Generally speaking, compounds **5a–f** possessing halide atom(s) on the benzene ring gave the inspiring inhibition rates between 55.9% and 99.7%. Especially, dichlorobenzyl **5f** and 2-trifloromethyl-4-fluorobenzyl **5g** gave the exciting inhibition of 99.7% and 98.1%, respectively. Meanwhile, the introduction of electron-withdrawing *o*-nitro (**5h**), *p*-methoxycarbonyl (**5i**), *p*-carboxylic acid (**5j**) and bulky 12*N*-cytisine (**5k**) only gave moderate improvements in activity. Therefore, it appeared that 12*N*-benzyl or methylene linker gave the highest enhancement on anti-COL1A1 activity.

In the next step, all compounds with the inhibition rates of over 50% at the concentration of 80 μM were selected to investigate their activity at the concentration of 40 μM. As indicated in Table 1, compounds **5c**, **5f** and **5g** displayed the highest rates of 74.5%, 86.4% and 81.7%, respectively, and thus were selected as the representative

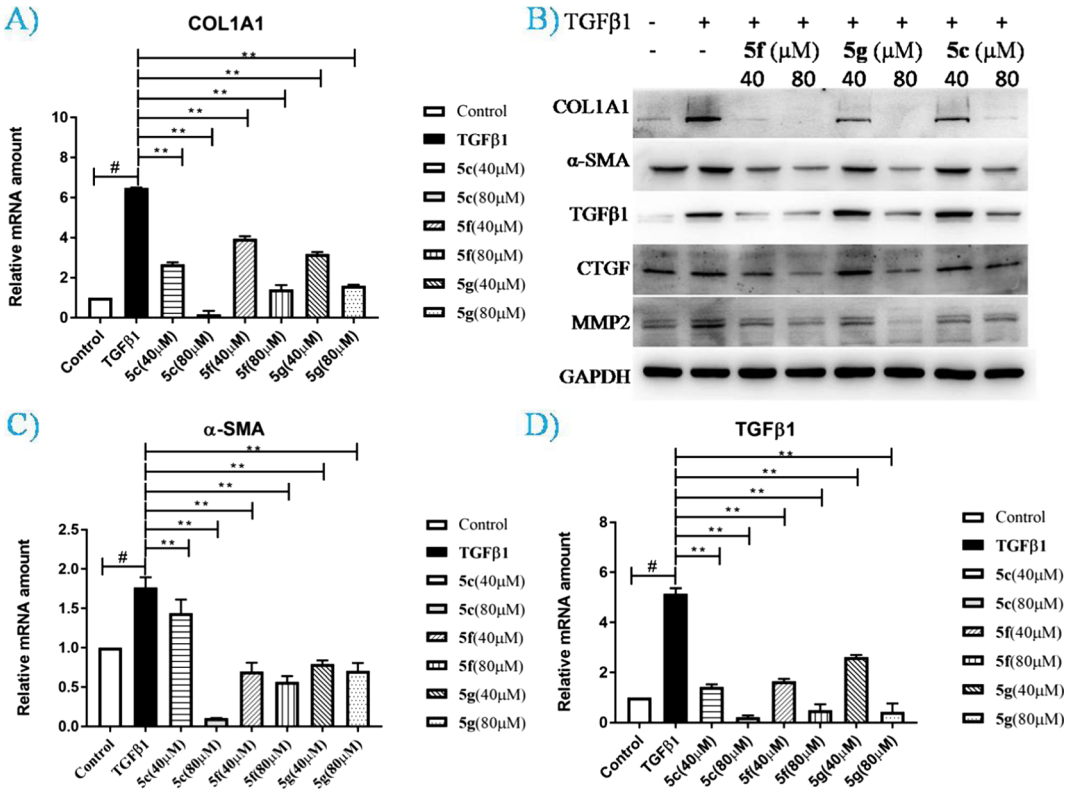

Fig. 2. (A) Effects of compounds **5c**, **5f** and **5g** inhibiting COL1A1 mRNA level. (B) Effects of compounds **5c**, **5f** and **5g** inhibiting fibrogenetic COL1A1, α-SMA, TFGβ1, CTGF and MMP2 proteins by Western Blot assay. (C) Effects of compounds **5c**, **5f** and **5g** inhibiting α-SMA mRNA levels. (D) Effects of compounds **5c**, **5f** and **5g** inhibiting TGFβ1 mRNA levels. The protein expression levels were normalized against GAPDH. Data analyzed by RT-PCR were presented as the mean ± SEM, (#) $p < 0.05$ as compared to that of control group; (**) $p < 0.01$ as compared to that of TGFβ1 group.

compounds to further evaluate their effancy by testing the half maximal inhibition concentration (IC_{50}) values on COL1A1 promotor expression, and they gave the IC_{50} values of 22.2, 12.8 and 16.9 μM, respectively. Then their cytotoxicities in HepG2 cell were tested. Compounds **5c** and **5f** displayed higher cellular safety profiles with the median cytotoxic concentration (CC_{50}) value of over 400 μM, while compound **5g** gave a CC_{50} value of 247.1 μM. Compound **5f** gave the highest selectivity index (SI, CC_{50}/IC_{50}) value of over 32.3, as indicated in Table 1.

2.3. Inhibition effects on the mRNA and protein expression of COL1A1

The inhibitory effects against COL1A1 of the three representative compounds **5c**, **5f** and **5g** were confirmed on both mRNA and protein levels. Their anti-COL1A1 effect on mRNA level was evaluated by real-time (RT) PCR amplification, and LX-2 cells were stimulated with TGFβ1 (2 ng/mL), and then treated with compounds **5c**, **5f** or **5g** (40 μM and 80 μM) respectively. As indicated in Fig. 2A, TGFβ1 treatment greatly enhanced the mRNA level of COL1A1, and the treatment of **5c**, **5f** and **5g** effectively reversed the enrichment in a dose-dependent manner, with the inhibitory rates of 69.6%, 46.1% and 60.3% at the concentration of 40 μM and 115.3%, 92.5% and 89.0% at the concentration of 80 μM, respectively.

Then their anti-COL1A1 effect on protein level was carried out by western blot assay. As indicated in Fig. 2B, 5c, 5f and 5g significantly reversed the increase of COL1A1 protein induced by TGFβ1 in a dose-dependent manner, and the generation of COL1A1 was suppressed almost completely in treatment of **5f** or **5g** at the concentration of 80 μM. These results suggested that these key compounds could effectively reduce COL1A1 expression on both mRNA and protein levels.

2.4. Inhibition effects on the mRNA and protein expression of α-SMA

Similarly, α-SMA expression in LX-2 cells on both mRNA and protein level were significantly stimulated by TGFβ1 treatment as anticipated, and the addition of **5c**, **5f** and **5g** substantially repressed this stimulation, as shown in Fig. 2B and C, respectively. Compounds **5c**, **5f** and **5g** reduced α-SMA mRNA level in a dose-dependent manner, with the inhibitory rates of 42.8%, 134% and 127% at the concentration of 40 μM and inhibition rates of 217%, 157% and 139% at the concentration of 80 μM, respectively. Western blot assay disclosed that **5c**, **5f** and **5g** reduced α-SMA protein level in a dose-dependent manner, by approximately 50% at the concentration of 80 μM. Thus, this kind of compounds also inhibited fibrogenetic α-SMA expression.

2.5. Inhibition effects on the protein expression of CTGF and MMP2

CTGF, a highly profibrogenic protein over-expressing in many fibrotic lesions, plays an important role in the pathogenesis of liver fibrosis [19,20], and MMP2 is another endogenous peptidase to degrade the basement membrane [21]. Therein, the effects on both CTGF and MMP-2 proteins under the stimulation of TGFβ1 of key compounds were respectively evaluated. As shown in Fig. 2B, upon single stimulation with TGFβ1, CTGF protein level increased (Fig. 2B), while the additions of **5c**, **5f** and **5g** (40 or 80 μm) dose-dependently suppressed TGFβ1-stimulated expression of CTGF. Also, a 2.5-fold increase of MMP2 protein level was witnessed upon single stimulation with TGFβ1, and the treatments of **5c**, **5f** and **5g** dose-dependently suppressed TGFβ1-stimulated expression of MMP2. These results suggested that all of them abolished TGF-β1-induced CTGF and MMP2 expressions in LX2 cells.

2.6. Inhibition effects on the mRNA and protein expression of TGFβ1

Since the stimulation of TGFβ1 provokes the expression of a series of fibrosis genes like COL1A1, α-SMA, CTGF, MMP2 as well as TGFβ1 itself [12,19–21], might the treatment of key compounds lead to a negative effect on TGFβ1 expression as well? As anticipated, the generation of TGFβ1 was also markedly induced by TGFβ1 treatment on both protein (Fig. 2B) and mRNA (Fig. 2D) levels. The addition of **5c**, **5f** and **5g** effectively inhibited the booming of TGFβ1 both on mRNA level (Fig. 2D) and protein level(Fig. 2B). RT-PCR analysis disclosed that **5c**, **5f** and **5g** significantly reduced TGFβ1 mRNA level in a dose-dependent manner, with the inhibitory rates of 89.6%, 84.2% and 60.9% at the concentration of 40 μM and inhibition rates of 119%, 112% and 114% at the concentration of 80 μM, respectively. Then it was speculated that these cytisine derivatives might inhibit both the progress of fibrosis and cascade enlargement effect of TGFβ1 stimulation.

2.7. Stability of key compounds in whole blood in vitro

To further evaluate the druglike property of its kind, the *in vitro* metabolic stability of compounds **5c**, **5f** and **5g** in whole blood was investigated, taking enalapril as the positive control [22]. As indicated in Fig. 3, enalapril displayed an expected low stability in blood due to the presence of a hydrolyzable ester bond, and the remaining rates of protype enalapril were 41.9% at 0.5 h, and 20.2% at 1 h, respectively. Compounds **5c**, **5f** and **5g** gave higher stability profiles in blood, and the remaining rates of **5c**, **5f** and **5g** were 85.2%, 96.7% and 82.2% at 1 h, and 67.1%, 87.7% and 61.7% at 8 h, respectively. The results indicated their high stability profiles in blood, and compounds **5f** owned the highest stability to metabolism *in vitro*.

2.8. Pharmacokinetic (PK) and safety profile assessments in vivo

Considering the possible metabolic instability caused by iodo substitution in **5c**, the *in vivo* PK behaviors of compound **5f** and **5g** were further investigated in adult male Sprague-Dawley (SD) rat model at the dosage of 25 mg/kg via oral route. As depicted in Table 2 and Fig. 4, compounds **5f** and **5g** demonstrated the C_{max} values of 960 and 220 nM and AUC values of 1120 and 730 nM•h, indicating **5f** owns a higher stability to metabolism *in vivo*.

To evaluate the safety profiles of **5c**, **5f** and **5g**, an acute toxicity test was performed in Kunming mice. Compounds were given orally in a single-dosing experiment at 125, 250 or 500 mg•kg^{-1}, respectively. The mice were closely monitored for 7 days. To our delight, during the experiment period, no abnormalities in weight, food intake or behavior of mice was observed in all group, and all these three compounds gave a median lethal dose (LD_{50}) value over 500 mg•kg^{-1}, indicating their good safety profiles *in vivo*.

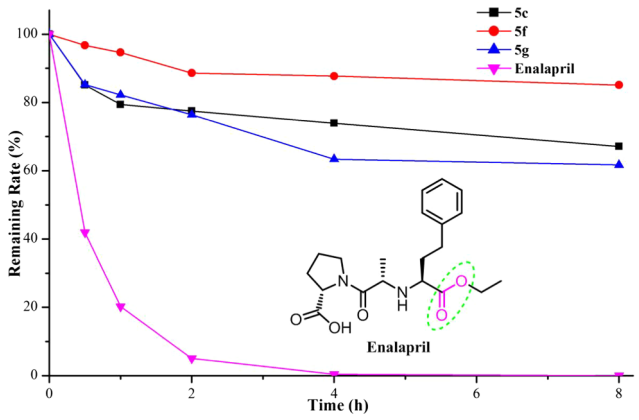

Fig. 3. Metabolic stability of compounds **5c**, **5f** and **5g** in whole blood.

2.9. Primary mechanism of action of key compounds

In view of the importance of TGFβ/Smad signaling pathway in activating HSCs and ECM formation during hepatic injury [23], the effects of key compounds on phosphorylated Smad levels was initiated. In this study, stimulation of TGFβ1 accelerated the phosphorylation of Smad2, and compounds **5c**, **5f** and **5g** repressed the booming of Smad2 phosphorylation in a dose-dependent manner, as depicted in Fig. 5A. Therefore, it was speculated that they might exert the anti-liver fibrotic activity via repressing the TGFβ/Smad pathway.

In liver, the PI3K/Akt signaling pathway has been well documented as an important pathway to regulate the proliferation and *trans*-differentiation of HSCs [24]. The activation of PI3K by growth factors in turn induces the phosphorylation of Akt and leads to the activation of HSCs [24]. Since the PI3K/Akt pathway is an upstream modulator of TGFβ1/Smad signaling process [18,25], the modulatory effects on PI3K/Akt pathway of the key compounds were investigated by western blot assay, and the results were indicated in Fig. 5B. All three compounds obviously repressed the phosphorylations of PI3K and Akt in LX-2 cells in a dose-dependent manner after TGFβ1 stimulation. Therefore, it was speculated that these compounds might exert the anti-fibrotic effect through the blocking of the PI3K/Akt signaling pathway, then down-regulating the phosphorylation of Smad2 [16], and down-regulating the expression of fibrogenetic proteins including COL1A1, α-SMA, TGFβ1, CTGA and MMP-2 in LX2 cells finally, as described in Fig. 6.

3. Conclusions

A total of twenty-six novel cytisine derivatives with a unique endocyclic scaffold were first synthesized and evaluated for suppression of COL1A1 promotor expression in LX2 cells. SAR indicated that introduction of a 12*N*-benzyl substitution might significantly enhanced the potency. Among them, compound **5f** exhibited promising inhibitory potency against COL1A1 with an IC_{50} value of 12.8 μM, and it also gave inspiring inhibition activities against COL1A1, α-SMA, TGFβ1, CTGA and MMP-2 on both mRNA and/or protein levels, indicating a wide range of activity against fibrogenetic proteins. Meanwhile, it displayed a high stability in whole blood and a high safety profile with the LD_{50} value of 500 mg•kg^{-1} orally. Preliminary mechanism of action demonstrated that compound **5f** targeted on PI3K/Akt/Smad pathway, thereby displaying extensive activity against several fibrogenetic proteins in LX2 cells. Therefore, we consider 12*N*-benzyl cytisine derivatives to be a novel promising class of anti-liver fibrosis agents worthy of further investigation.

4. Experimental section

4.1. Chemistry

4.1.1. General experimental information

Unless otherwise noted, all commercial reagents and solvents were obtained from the commercial provider and used without further purification. Melting points (mp) were obtained with a MP90 melting point apparatus and were uncorrected (Mettler-Toledo, Greifensee, Switzerland). ^{1}H NMR and ^{13}C NMR spectra were recorded on a Bruker Avance III 500 and 600 spectrometers (Varian, San Francisco, USA) in DMSO-d_6 with Me_4Si as the internal standard. Chemical shifts are referenced to the residual solvent peak and reported in ppm (δ scale) and all coupling constant (*J*) values are given in Hz. ESI high-resolution mass spectra (HRMS) were recorded on an Autospec Ultima-TOF spectrometer (Micromass UK Ltd., Manchester, U.K.). Flash chromatography was performed on Combiflash Rf 200 (Teledyne, Nebraska, USA).

4.1.2. General procedures for 12N-benzoylcytisine derivatives (1a–c)

To a solution of cytisine (2 mmol) in dichloromethane (30 mL), triethylamine (2.4 mmol), and the substituted benzoyl chloride

Table 2
PK Profiles and LD_{50} Values of Key Compounds *in vivo*.

Code	LD_{50} (mg/kg)	T_{max} (h)	C_{max} (nM)	AUC_{0-t} (nM·h)	MRT (h)	$t_{1/2}$ (h)
5c	> 500	NT	NT	NT	NT	NT
5f	> 500	0.25 ± 0	960 ± 20	1120 ± 250	1.73 ± 0.34	1.30 ± 0.24
5g	> 500	0.50 ± 0	220 ± 50	730 ± 40	2.62 ± 0.18	1.56 ± 0.96

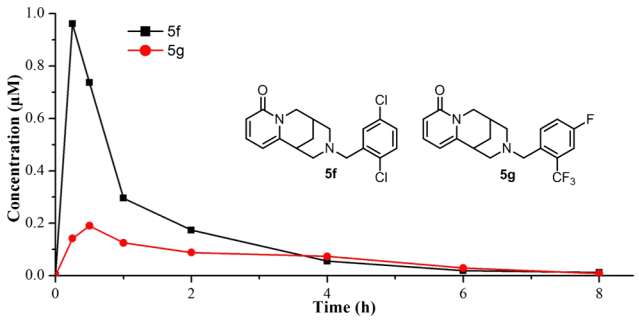

Fig. 4. Plasma concentration of **5f** and **5g** after PO dosing at 25 mg/kg.

(2.2 mmol) were added and stirred at room temperature until the TLC analysis showed completion of the reaction. Then the reaction solution was washed with water and brine. The organic phase was dried with anhydrous sodium sulfate and concentrated to give a residue, which was purified by flash column chromatography on silica gel with CH_2Cl_2/CH_3OH as the eluent and then acidified with 2 N HCl/Et_2O to give the title compounds.

*4.1.2.1. 12N-3′-Methoxybenzoylcytisine (**1a**).* The title compound was prepared from cytisine and *m*-methoxybenzoyl chloride in the same manner as described above. Yield: 68%; white solid; mp: 140–142 °C. ^{1}H NMR (600 MHz) δ 7.32 (s, 1H), 7.19 (s, 1H), 6.93 (s, 1H), 6.70–5.81 (m, 4H), 4.81–4.31 (m, 1H), 4.11–3.75 (m, 2H), 3.70 (s, 3H), 3.63–3.34 (m, 2H), 3.24–2.91 (m, 2H), 2.33 (s, 1H), 1.99–1.92 (m, 2H); ^{13}C NMR (151 MHz) δ 169.9, 162.6, 159.4, 149.9, 139.5, 129.8, 118.6, 116.5, 115.6 (2), 111.7, 105.3, 55.6, 54.5, 49.0, 48.0, 34.5, 27.5, 25.7. HRMS: calcd for $C_{19}H_{21}N_2O_3$ $[M+H]^+$ 325.1547, found: 325.1544.

*4.1.2.2. 12N-3′,5′-Dimethoxybenzoylcytisine (**1b**).* The title compound was prepared from cytisine and 3,5-dimethoxybenzoyl chloride in the same manner as described above. Yield: 62%; white solid; mp: 113–115 °C. ^{1}H NMR (600 MHz) δ 7.32 (s, 1H), 6.47 (s, 1H), 6.30 (d, J = 8.4 Hz, 1H), 6.26–5.82 (m, 3H), 4.78–4.36 (m, 1H), 3.96 (s, 1H), 3.69 (s, 6H), 3.63–3.37 (m, 2H), 3.32–2.87 (m, 3H), 2.34 (s, 1H), 1.97–1.94 (m, 2H); ^{13}C NMR (151 MHz) δ 169.8, 162.6, 160.7, 145.0, 139.6, 116.4 (2), 105.3, 104.2 (2), 101.6 (2), 55.8 (2), 54.4, 49.0, 47.9, 34.5, 27.4, 25.7. HRMS: calcd for $C_{20}H_{23}N_2O_4$ $[M+H]^+$ 355.1652, found: 355.1642.

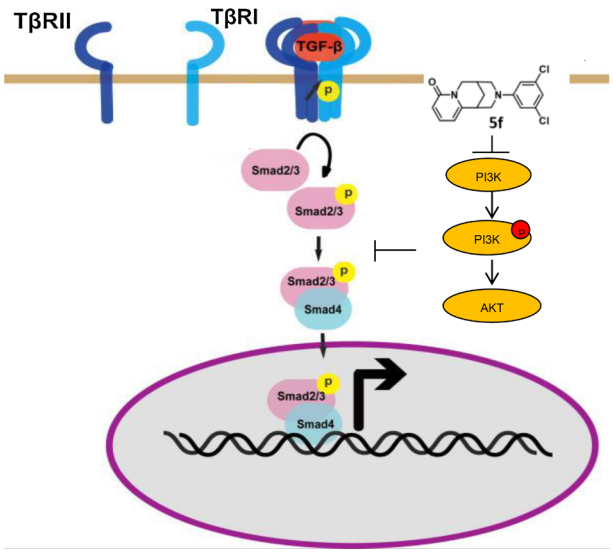

Fig. 6. Cartoon signaling pathway of compound **5f** against liver fibrosis in LX2 cells.

*4.1.2.3. 12N-4′-Fluoro-3′-trifluoromethylbenzoylcytisine (**1c**).* The title compound was prepared from cytisine and 4-fluoro-3-trifluoromethylbenzoyl chloride in the same manner as described above. Yield: 50%; white solid; mp: 134–136 °C. ^{1}H NMR (600 MHz) δ 7.76–6.91 (m, 4H), 6.38–5.84 (m, 2H), 4.79–4.41 (m, 1H), 4.03 (s, 1H), 3.89–3.41 (m, 3H), 3.06 (s, 2H), 2.54 (s, 1H), 2.02–1.94 (m, 2H); ^{13}C NMR (151 MHz) δ 167.9, 162.6, 160.3, 158.6, 149.8, 139.4, 133.7 (2), 125.8, 123.5, 121.7, 116.5, 105.1, 54.9, 49.1, 48.2, 34.6, 27.5, 25.6. HRMS: calcd for $C_{19}H_{17}F_4N_2O_2$ $[M+H]^+$ 381.1221, found: 381.1255.

*4.1.3. Synthesis of 12N-2′-furoylcytisine (**1d**)*

To a solution of cytisine (2 mmol) in dichloromethane (30 mL), triethylamine (2.4 mmol), and 2-furoyl chloride (2.2 mmol) were added and stirred at room temperature until the TLC analysis showed completion of the reaction. Then the reaction solution was washed with water and brine. The organic phase was dried with anhydrous sodium sulfate and concentrated to give a residue, which was purified by flash column chromatography on silica gel with CH_2Cl_2/CH_3OH as the eluent

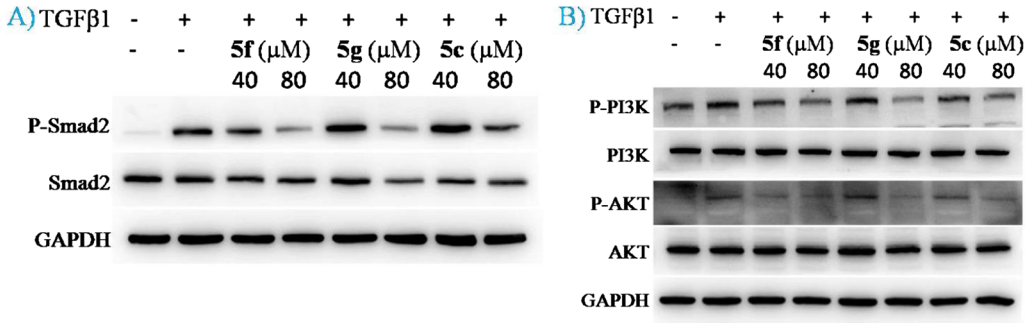

Fig. 5. Compounds **5c**, **5f** and **5g** reduced the expression of A) members of the TGFβ1/Smad signaling pathway. (B) members of the PI3K/Akt signaling pathway. The protein expression levels were normalized against GAPDH.

and then acidified with 2 N HCl/Et_2O to give the title compounds. Yield: 50%; white solid; mp: 151–153 °C. ^{1}H NMR (600 MHz) δ 7.74 (s, 1H), 7.29 (dd, J = 9.0, 4.8 Hz, 1H), 6.68 (s, 1H), 6.53 (s, 1H), 6.19 (d, J = 9.0 Hz, 1H), 6.13 (d, J = 4.8 Hz, 1H), 4.47 (s, 1H), 4.29 (s, 1H), 3.93–3.67(m, 2H), 3.60–3.35 (m, 1H), 3.30–2.83 (m, 3H), 2.02–1.94 (m, 2H); ^{13}C NMR (151 MHz) δ 162.6, 159.5, 145.0, 147.0, 145.0, 139.3, 116.5, 115.6, 111.6, 105.1, 48.9, 34.5, 27.5 (2), 25.8 (2). HRMS: calcd for $C_{16}H_{17}N_2O_3$ $[M+H]^+$ 285.1234, found: 285.1233.

*4.1.4. Synthesis of 12N-4′-methoxycarbonylbenzenesulfonylcytisine (**2a**)*

To a solution of cytisine (2 mmol) in dichloromethane (30 mL), triethylamine (2.4 mmol), and 4-methoxycarbonyl benzenesulfonyl chloride (2.2 mmol) were added and stirred at room temperature until the TLC analysis showed completion of the reaction. Then the reaction solution was washed with water and brine. The organic phase was dried with anhydrous sodium sulfate and concentrated to give a residue, which was purified by flash column chromatography on silica gel with CH_2Cl_2/CH_3OH as the eluent and then acidified with 2 N HCl/Et_2O to give the title compounds. Yield: 85%; white solid; mp: 112–114 °C. ^{1}H NMR (600 MHz) δ 7.73 (t, J = 6.0 Hz, 1H), 7.68–7.62 (m, 2H), 7.59 (d, J = 7.2 Hz, 1H), 7.36 (dd, J = 8.4, 7.2 Hz, 1H), 6.24 (d, J = 8.4 Hz, 1H), 6.18 (d, J = 6.0 Hz, 1H), 3.84 (s, 1H), 3.81 (s, 3H), 3.78–3.70 (m, 2H), 3.65–3.64 (m, 1H), 3.19 (s, 1H), 2.92–2.81 (m, 2H), 2.52 (s, 1H), 1.85–1.78 (m, 2H); ^{13}C NMR (151 MHz) δ 168.2, 162.5, 150.1, 139.5, 134.4, 133.5, 133.4, 131.2, 128.9, 128.6, 116.6, 105.2, 53.3, 53.1, 52.1, 49.0, 33.8, 26.8, 24.3. HRMS: calcd for $C_{19}H_{21}N_2O_5S$ $[M+H]^+$ 389.1166, found: 389.1155.

*4.1.5. Synthesis of 12N-5′-bromothiophenesulfonylcytisine (**2b**)*

To a solution of cytisine (2 mmol) in dichloromethane (30 mL), triethylamine (2.4 mmol), and 5-bromothiophenesulfonyl chloride (2.2 mmol) were added and stirred at room temperature until the TLC analysis showed completion of the reaction. Then the reaction solution was washed with water and brine. The organic phase was dried with anhydrous sodium sulfate and concentrated to give a residue, which was purified by flash column chromatography on silica gel with CH_2Cl_2/CH_3OH as the eluent and then acidified with 2 N HCl/Et_2O to give the title compounds. Yield: 46%; white solid; mp: 208–210 °C. ^{1}H NMR (600 MHz) δ 7.42 (s, 2H), 7.36 (dd, J = 9.0, 7.2 Hz, 1H), 6.26 (dd, J = 9.0, 1.2 Hz, 1H), 6.18–6.16 (m, 1H), 3.81–3.74 (m, 2H), 3.67–3.54 (m, 2H), 3.20 (s, 1H), 2.81–2.74 (m, 2H), 2.55 (s, 1H), 1.85–1.77 (m, 2H); ^{13}C NMR (151 MHz) δ 162.6, 145.0, 139.4, 137.0, 134.1, 132.4, 120.1, 116.7, 105.0, 53.2, 52.2, 49.2, 33.5, 26.7, 24.1. HRMS: calcd for $C_{15}H_{16}BrN_2O_3S_2$ $[M+H]^+$ 416.9760, found:416.9746.

*4.1.6. General procedures for 12N-carbamoylcytisine derivatives (**3a–g**)*

To a solution of cytisine (2 mmol) in dichloromethane (30 mL), the substituted isocyanate (2.2 mmol) were dropwise added and stirred at room temperature until the TLC analysis showed completion of the reaction. Then the reaction solution was washed with water and brine. The organic phase was dried with anhydrous sodium sulfate and concentrated to give a residue, which was purified by flash column chromatography on silica gel with CH_2Cl_2/CH_3OH as the eluent and then acidified with 2 N HCl/Et_2O to give the title compounds.

*4.1.6.1. 12N-2′,4′-Difluorophenylcarbamoylcarbamoylcytisine (**3a**).* The title compound was prepared from cytisine and 2,4-difluorophenyl isocyanate in the same manner as described above. Yield: 52%; white solid; mp: 193–195 °C; ^{1}H NMR (600 MHz) δ 8.13 (s, 1H), 7.33 (dd, J = 9.0, 6.6 Hz, 1H), 7.19–7.14 (m, 1H), 7.14–7.09 (m, 1H), 6.97–6.92 (m, 1H), 6.23 (dd, J = 9.0, 1.2 Hz, 1H), 6.18–6.14 (m, 1H), 4.25–4.23 (m, 1H), 4.10–4.09 (m, 1H), 4.06–4.03 (m, 1H), 3.69–3.68 (m, 1H), 3.18–3.04 (m, 3H), 2.45 (s, 1H), 1.92 (d, J = 2.4 Hz, 2H); ^{13}C NMR (151 MHz) δ 162.7, 159.1, 156.1, 155.6, 150.5, 139.3, 128.3, 124.3, 116.2, 111.1, 105.2, 104.3, 51.3, 50.2, 48.9, 34.4, 27.4, 25.6. HRMS: calcd for $C_{18}H_{18}F_2N_3O_2$ $[M+H]^+$ 346.1362, found: 346.1354.

*4.1.6.2. 12N-2′-Fluoro-5′-trifluoromethylcarbamoylcytisine (**3b**).* The title compound was prepared from cytisine and 2-fluoro-5-trifluoromethylphenyl isocyanate in the same manner as described above. Yield: 50%; white solid; mp: 160–162 °C; ^{1}H NMR (600 MHz) δ 8.42 (br, 1H), 7.57 (d, J = 7.2 Hz, 1H), 7.37–7.32 (m, 3H), 6.21–6.17 (m, 2H), 4.29–4.26 (m, 1H), 4.13–4.10 (m, 2H), 3.69–3.68 (m, 1H), 3.20–3.10 (m, 3H), 2.46 (s, 1H), 1.97–1.92 (m, 2H); ^{13}C NMR (151 MHz) δ 162.6, 157.0, 155.2, 150.3, 139.3, 129.1, 125.3, 124.2, 122.8, 122.0, 117.0, 116.2, 105.3, 51.6, 50.3, 48.9, 34.5, 27.4, 25.6. HRMS: calcd for $C_{19}H_{18}F_4N_3O_2$ $[M+H]^+$ 396.1330, found: 396.1320.

*4.1.6.3. 12N-2′-Trifluoromethylphenylcarbamoylcytisine (**3c**).* The title compound was prepared from cytisine and 2-trifluoromethylphenyl isocyanate in the same manner as described above. Yield: 78%; white solid; mp: 187–189 °C; ^{1}H NMR (600 MHz) δ 8.01 (s, 1H), 7.61 (d, J = 7.8 Hz, 1H), 7.55 (t, J = 7.8 Hz, 1H), 7.36–7.31 (m, 2H), 7.15 (d, J = 7.8 Hz, 1H), 6.25 (dd, J = 9.0, 1.2 Hz, 1H), 6.15 (d, J = 6.6 Hz, 1H), 4.23–4.21 (m, 1H), 4.10–4.08 (m, 1H), 4.02–4.00 (m, 1H), 3.71–3.69 (m, 1H), 3.14–3.06 (m, 3H), 2.46 (s, 1H), 1.96–1.89 (m, 2H); ^{13}C NMR (151 MHz) δ 162.7, 156.1, 150.5, 139.3, 137.7, 132.9, 130.8, 126.5, 126.3, 125.9, 124.1, 116.2, 105.1, 51.1, 50.1, 48.9, 34.4, 27.3, 25.6. HRMS: calcd for $C_{19}H_{19}F_3N_3O_2$ $[M+H]^+$ 378.1424, found: 378.1420.

*4.1.6.4. 12N-4′-Trifluoromethyloxophenylcarbamoylcytisine (**3d**).* The title compound was prepared from cytisine and 4-trifluoromethyloxophenyl isocyanate in the same manner as described above. Yield: 56%; white solid; mp: 197–199 °C; ^{1}H NMR (600 MHz) δ 8.53 (s, 1H), 7.39–7.33 (m, 2H), 7.32–7.30 (m, 1H), 7.17 (d, J = 9.0 Hz, 2H), 6.21–6.14 (m, 2H), 4.29–4.26 (m, 1H), 4.14–4.12 (m, 1H), 4.07–4.05 (m, 1H), 3.71–3.68 (m, 1H), 3.16–3.05 (m, 3H), 2.47 (s, 1H), 1.92 (s, 2H); ^{13}C NMR (151 MHz) δ 162.6, 155.5, 150.5, 143.1, 140.0, 139.3, 121.5 (2), 121.5, 121.3 (2), 116.2, 105.1, 51.2, 50.3, 48.9, 34.4, 27.4, 25.6. HRMS: calcd for $C_{19}H_{19}F_3N_3O_3$ $[M+H]^+$ 394.1373, found: 394.1366.

*4.1.6.5. 12N-3′,5′-Dimethylphenylcarbamoylcytisine (**3e**).* The title compound was prepared from cytisine and 3,5-dimethylphenyl isocyanate in the same manner as described above. Yield: 32%; white solid; mp: above 250 °C. ^{1}H NMR (600 MHz) δ 8.18 (s, 1H), 7.31 (dd, J = 9.0, 7.2 Hz, 1H), 6.89 (s, 2H), 6.54 (s, 1H), 6.19 (dd, J = 9.0, 1.2 Hz, 1H), 6.15–6.12 (m, 1H), 4.26–4.24 (m, 1H), 4.12–4.09 (m, 1H), 4.06–4.03 (m, 1H), 3.71–3.67 (m, 1H), 3.12 (s, 1H), 3.07–3.01 (m, 2H), 2.45 (s, 1H), 2.16 (s, 6H), 1.90 (s, 2H); ^{13}C NMR (151 MHz) δ 162.1, 155.1, 150.1, 139.9, 138.8, 136.9 (2), 123.3, 117.6 (2), 115.6, 104.5, 50.6, 49.7, 48.4, 33.8, 26.8, 25.0, 20.9 (2). HRMS: calcd for $C_{20}H_{24}N_3O_2$ $[M+H]^+$ 338.1863, found: 338.1856.

*4.1.6.6. 12N-Isopropylcarbamoylcytisine (**3f**).* The title compound was prepared from cytisine and 4-fluoro-3-trifluoromethylbenzoyl chloride in the same manner as described above. Yield: 52%; white solid; mp: above 250 °C. ^{1}H NMR (600 MHz) δ 7.31 (dd, J = 9.0, 6.6 Hz, 1H), 6.19 (dd, J = 9.0, 1.2 Hz, 1H), 6.11 (dd, J = 6.6, 1.2 Hz, 1H), 5.97 (d, J = 7.2 Hz, 1H), 4.10–4.08 (m, 1H), 3.99–3.98 (m, 1H), 3.93–3.91 (m, 1H), 3.65–3.62 (m, 1H), 3.60–3.54 (m, 1H), 3.04 (s, 1H), 2.93–2.91 (m, 1H), 2.88–2.86 (m, 1H), 2.37 (s, 1H), 1.85 (s, 2H), 0.92 (d, J = 6.0 Hz, 3H), 0.88 (d, J = 6.6 Hz, 3H); ^{13}C NMR (151 MHz) δ 162.6, 157.2, 150.9, 139.2, 116.1, 105.0, 50.9, 49.95, 49.0, 42.1, 34.4, 27.4, 25.8, 23.3, 23.2. HRMS: calcd for $C_{15}H_{22}N_3O_2$ $[M+H]^+$ 276.1707, found: 276.1704.

*4.1.6.7. 12N-Cyclopentylcarbamoylcytisine (**3 g**).* The title compound was prepared from cytisine and 4-fluoro-3-trifluoromethylbenzoyl chloride in the same manner as described above. Yield: 55%; white solid; mp: 180–182 °C; ^{1}H NMR (600 MHz) δ 7.36–7.27 (m, 1H), 6.19 (d, J = 9.0 Hz, 1H), 6.10 (d, J = 6.6 Hz, 1H), 6.02 (d, J = 5.4 Hz, 1H),

4.12–4.10 (m, 1H), 4.00–3.97 (m, 1H), 3.93–3.91 (m, 1H), 3.76–3.68 (m, 1H), 3.66–3.65 (m, 1H), 3.04 (s, 1H), 2.93–2.91 (m, 1H), 2.87–2.85 (m, 1H), 2.37 (s, 1H), 1.85 (s, 2H), 1.70–1.45 (m, 4H), 1.38 (d, J = 6.0 Hz, 2H), 1.25 (d, J = 4.8 Hz, 1H), 1.17 (d, J = 4.8 Hz, 1H); ^{13}C NMR (151 MHz) δ 162.6, 157.7, 150.9, 139.2, 116.1, 105.0, 52.3, 51.0, 50.0, 49.0, 34.4, 32.9, 32.6, 27.3, 25.7, 23.9, 23.8. HRMS: calcd for $C_{17}H_{24}N_3O_2$ $[M+H]^+$ 302.1863, found: 302.1857.

*4.1.7. General procedures for 12N-thiocarbamoylcytisine derivatives (**4a–b**)*

To a solution of cytisine (2 mmol) in dichloromethane (30 mL), the substituted phenyl isothiocyanate (2.2 mmol) were dropwise added and stirred at room temperature until the TLC analysis showed completion of the reaction. Then the reaction solution was washed with water and brine. The organic phase was dried with anhydrous sodium sulfate and concentrated to give a residue, which was purified by flash column chromatography on silica gel with CH_2Cl_2/CH_3OH as the eluent and then acidified with 2 N HCl/Et_2O to give the title compounds.

*4.1.7.1. 12N-2′-Methylthiophenylthiocarbamoylcytisine (**4a**)*. The title compound was prepared from cytisine and 2-methylthiophenyl isothiocyanate in the same manner as described above. Yield: 77%; white solid; mp: 245 °C (dec.). ^{1}H NMR (600 MHz) δ 8.88 (s, 1H), 7.29–7.27 (m, 1H), 7.20–7.15 (m, 2H), 7.08–7.04 (m, 1H), 6.89 (d, J = 7.8 Hz, 1H), 6.27 (dd, J = 9.0, 1.2 Hz, 1H), 6.17–6.12 (m, 1H), 5.19–5.18 (m, 1H), 5.02–5.00 (m, 1H), 4.25–4.22 (m, 1H), 3.75–3.74 (m, 1H), 3.33–3.31 (m, 1H), 3.26–3.23 (m, 1H), 3.20 (s, 1H), 2.59 (s, 1H), 2.27 (s, 3H), 2.08–2.06 (m, 1H), 2.00–1.97 (m, 1H); ^{13}C NMR (151 MHz) δ 182.1, 161.9, 148.4, 138.0, 137.7, 137.3, 128.7, 126.3, 125.0, 123.9, 115.7, 104.6, 53.5, 52.7, 47.6, 34.3, 27.4, 25.2, 14.3. HRMS: calcd for $C_{19}H_{22}N_3OS_2$ $[M+H]^+$ 372.1199, found: 372.1192.

*4.1.7.2. 12N-2′-Methoxy-4′-nitrophenylthiocarbamoylcytisine (**4b**)*. The title compound was prepared from cytisine and 2-methoxy-4-nitrophenyl isothiocyanate in the same manner as described above. Yield: 42%; white solid; mp: above 250 °C. ^{1}H NMR (600 MHz) δ 8.80 (s, 1H), 7.74 (dd, J = 12.0, 9.0 Hz, 2H), 7.33–7.31 (m, 1H), 7.19 (d, J = 9.0 Hz, 1H), 6.28–6.27 (m, 1H), 6.15 (d, J = 6.0 Hz, 1H), 5.11–5.09 (m, 1H), 4.80–4.78 (m, 1H), 4.16–4.13 (m, 1H), 3.83 (s, 3H), 3.69–3.68 (m, 1H), 3.42–3.41 (m, 1H), 3.30 (s, 1H), 3.22 (s, 1H), 2.58 (s, 1H), 2.07–2.05 (m, 1H), 1.95–1.92 (m, 1H); ^{13}C NMR (151 MHz) δ 182.5, 162., 152.7, 149.6, 144.5, 139.2, 137.4, 126.4, 116.6, 116.0, 106.8, 105.3, 56.6, 55.6, 54.1, 48.6, 35.1, 28.4, 25.8. HRMS: calcd for $C_{19}H_{21}N_4O_4S$ $[M+H]^+$ 401.1278, found: 401.1273.

*4.1.8. General procedures for 12N-benzylcytisine derivatives (**5a–i**)*

To a solution of cytisine (2 mmol) in acetonitrile (30 mL), K_2CO_3 (3 mmol) and the substituted benzyl halide (3 mmol) were added and stirred at room temperature until the TLC analysis showed completion of the reaction, then filtered. The filtrate was evaporated, and the residue was dissolved with CH_2Cl_2, washed with water, brine, dried. It was then filtered and concentrated to give a residue, which was purified by flash column chromatography on silica gel with CH_2Cl_2/CH_3OH as the eluent and then acidified with 2 N HCl/Et_2O to give the title compounds.

*4.1.8.1. 12N-2′-Chlorobenzylcytosine hydrochloride (**5a**)*. The title compound was prepared from cytisine and 3-chlorobenzyl bromide in the same manner as described above. Yield: 54%; white solid; mp: 223–225 °C. ^{1}H NMR (500 MHz) δ 10.20 (s, 1H), 7.73 (s, 1H), 7.58 (d, J = 6.6 Hz, 1H), 7.53 (d, J = 8.0 Hz, 1H), 7.50–7.46 (m, 1H), 7.44–7.41 (m, 1H), 6.41 (d, J = 9.0 Hz, 1H), 6.28 (d, J = 6.6 Hz, 1H), 4.38–4.36 (m, 1H), 4.32–4.31 (m, 1H), 4.00–3.96 (m, 1H), 3.86–3.82 (m, 1H), 3.49–3.48 (m, 1H), 3.42 (s, 1H), 3.31 (s, 1H), 3.21–3.19 (m, 1H), 2.77 (s, 1H), 1.94–1.92 (m, 1H), 1.87–1.84 (d, 1H); ^{13}C NMR (151 MHz) δ 162.7, 148.0, 140.1, 133.59, 132.3, 132.0, 131.2, 131.0, 130.1, 117.2, 107.2, 59.5, 56.5, 56.3, 48.5, 32.4, 26.3, 23.0. HRMS: calcd for $C_{18}H_{19}ClN_2O$·HCl [M-HCl + H]$^+$ 315.1259, found: 315.1250.

*4.1.8.2. 12N-2′-Bromobenzylcytosine (**5b**)*. The title compound was prepared from cytisine and 2-bromobenzyl bromide in the same manner as described above. Yield: 57%; white solid; mp: 129–131 °C. ^{1}H NMR (500 MHz) δ 7.51 (dd, J = 7.2, 1.2 Hz, 1H), 7.34–7.30 (m, 1H), 7.14 (m, 2H), 6.93–6.91 (m, 1H), 6.25–6.23 (m, 1H), 6.03 (d, J = 7.2 Hz, 1H), 3.83–3.80 (m, 1H), 3.70–3.66 (m, 1H), 3.48–3.40 (m, 2H), 3.01 (s, 1H), 2.88–2.86 (m, 1H), 2.77–2.72 (m, 1H), 2.43–2.34 (m, 3H), 1.86–1.83 (m, 1H), 1.75–1.72 (m, 1H); ^{13}C NMR (126 MHz) δ 162.9, 152.6, 139.3, 137.8, 133.2, 130.7, 129.4, 127.8, 124.2, 116.0, 104.4, 61.2, 60.5, 60.2, 50.2, 35.2, 28.1, 25.7. HRMS: calcd for $C_{18}H_{20}BrN_2O$ $[M+H]^+$ 359.0753, found: 359.0743.

*4.1.8.3. 12N-4′-Iodobenzylcytisine (**5c**)*. The title compound was prepared from 4 to iodobenzyl bromide in the same manner as described above. Yield: 60%; white solid; mp: 169–171 °C. ^{1}H NMR (600 MHz) δ 7.75 (dd, J = 7.8, 1.2 Hz, 1H), 7.29 (dd, J = 9.0, 7.2 Hz, 1H), 7.20–7.16 (m, 1H), 6.97–6.90 (m, 2H), 6.23 (dd, J = 9.0, 1.2 Hz, 1H), 6.01–6.00 (m, 1H), 3.79–3.76 (m, 1H), 3.70–3.67 (m, H), 3.39–3.31 (m, 2H), 3.00 (s, 1H), 2.84 (d, J = 8.4 Hz, 1H), 2.76–2.71 (m, 1H), 2.40–2.34 (m, 3H), 1.85–1.82 (m, 1H), 1.75–1.74 (m, 1H); ^{13}C NMR (151 MHz) δ 162.7, 152.4, 140.5, 139.6, 139.0, 130.4, 129.5, 128.2, 115.9, 104.2, 100.4, 65.5, 60.2, 59.8, 50.1, 35.0, 27.9, 25.6. HRMS: calcd for $C_{18}H_{20}IN_2O$ $[M+H]^+$ 407.0614, found: 407.0602.

*4.1.8.4. 12N-2′,5′-Difluorobenzylcytisine hydrochloride (**5d**)*. The title compound was prepared from cytisine and 2,5-difluorobenzyl bromide in the same manner as described above. Yield: 68%; white solid; mp: above 250 °C. ^{1}H NMR (600 MHz) δ 10.28 (s, 1H), 7.81–7.27 (m, 4H), 6.35 (d, J = 9.0 Hz, 1H), 6.24 (s, 1H), 4.30 (s, 2H), 3.98–3.95 (m, 1H), 3.83–3.80 (m, 1H), 3.44 (m, 5H), 2.72 (s, 1H), 1.94 (s, 1H), 1.83–1.81 (m, 1H); ^{13}C NMR (101 MHz) δ 162.8, 159.3, 156.9, 139.7 (3), 120.2, 118.0, 117.8, 117.4, 106.5, 56.4, 53.3 (2), 48.4, 32.6, 26.4, 22.9. HRMS: calcd for $C_{18}H_{19}F_2N_2O$·HCl $[M-HCl+H]^+$ 317.1460, found: 317.1454.

*4.1.8.5. 12N-2′-Chloro-5′-fluorobenzylcytisine (**5e**)*. The title compound was prepared from cytisine and 2-chloro-5-fluorobenzyl bromide in the same manner as described above. Yield: 72%; white solid; mp: 126–128 °C. ^{1}H NMR (600 MHz) δ 7.34 (dd, J = 9.0, 6.0 Hz, 1H), 7.28 (d, J = 3.0 Hz, 1H), 7.16 (t, J = 9.0 Hz, 1H), 6.85 (d, J = 3.0 Hz, 1H), 6.26 (d, J = 9.0 Hz, 1H), 6.05 (d, J = 6.0 Hz, 1H), 3.89–3.87 (m, 1H), 3.71 (dd, J = 9.0, 6.0 Hz, 1H), 3.55–3.42 (m, 2H), 2.29–2.27 (m, 1H), 1.85–1.83 (m, 1H), 1.72–1.70 (m, 1H); ^{13}C NMR (151 MHz) δ 162.6, 160.4, 158.7, 152.2, 139.3, 129.8, 128.7, 127.5, 117.4, 115.9, 104.2, 60.0, 59.8, 53.5, 50.1, 34.9, 28.0, 25.4. HRMS: calcd for $C_{18}H_{19}ClFN_2O$ $[M+H]^+$ 333.1165, found: 333.1159.

*4.1.8.6. 12N-2′,5′-Dichlorobenzylcytisine (**5f**)*. The title compound was prepared from cytisine and 2,5-dichlorobenzyl bromide in the same manner as described above. Yield: 67%; white solid; mp: 177–179 °C. ^{1}H NMR (500 MHz) δ 7.39–7.32 (m, 2H), 7.26 (dd, J = 8.4, 2.4 Hz, 1H), 6.85 (d, J = 2.4 Hz, 1H), 6.27–6.25 (m, 1H), 6.07–6.05 (m, 1H), 3.90–3.87(m, 1H), 3.73–3.70 (m, 1H), 3.48 (m, 2H), 3.02 (s, 1H), 2.94–2.92 (m, 1H), 2.74–2.69 (m, 1H), 2.51–2.51 (m, 1H), 2.43–2.42 (m, 1H), 2.34–2.31 (m, 1H), 1.86–1.85 (m, 1H), 1.76–1.75 (m, 1H); ^{13}C NMR (126 MHz) δ 162.8, 152.3, 139.5, 138.7, 132.4, 131.9, 131.4, 129.5, 128.7, 116.1, 104.4, 60.5, 60.3, 58.0, 50.3, 35.1, 28.2, 25.7. HRMS: calcd for $C_{18}H_{19}Cl_2N_2O$ $[M+H]^+$ 349.0869, found: 349.0860.

*4.1.8.7. 12N-4′-Fluoro-2′-trifluoromethylbenzylcytisine (**5g**)*. The title compound was prepared from cytisine and 4-fluoro-2-trifluoromethyl benzyl bromide in the same manner as described above. Yield: 64%; white solid; mp: 110–112 °C. ^{1}H NMR (600 MHz) δ 7.50 (dd, J = 10.8,

3.0 Hz, 1H), 7.33 (dd, J = 10.8, 9.0 Hz, 1H), 7.29–7.24 (m, 1H), 7.15–7.10 (m, 1H), 6.26 (d, J = 10.8 Hz, 1H), 6.01 (d, J = 7.8 Hz, 1H), 3.85–3.84 (m, 1H), 3.72–3.70 (m, 1H), 3.54–3.53 (m, 1H), 3.49–3.48 (m, 1H), 3.01 (s, 1H), 2.88–2.87 (m, 1H), 2.68–2.66 (m, 1H), 2.41–2.40 (m, 2H), 2.34–2.32 (m, 1H), 1.86–1.84 (m, 1H), 1.76–1.74 (m, 1H); ^{13}C NMR (151 MHz) δ 162.6, 161.3, 152.2, 139.1, 134.1, 132.7, 129.3, 123.8, 119.4, 115.8, 113.7, 104.2, 60.2 (2), 57.0, 50.0, 34.9, 27.9, 25.5. HRMS: calcd for $C_{19}H_{19}F_4N_2O$ $[M+H]^+$ 367.1428, found: 367.1418.

*4.1.8.8. 12N-2′-Nitrobenzylcytisine hydrochloride (**5h**)*. The title compound was prepared from cytisine and 2-nitrobenzyl bromide in the same manner as described above. Yield: 62%; white solid; mp: 188–190 °C. ^{1}H NMR (600 MHz) δ 10.51 (br, 1H), 8.29 (d, J = 9.0 Hz, 2H), 7.91 (s, 2H), 7.48–7.45 (m, 1H), 6.47 (d, J = 9.0 Hz, 1H), 6.32 (d, J = 6.6 Hz, 1H), 4.58–4.39 (m, 2H), 4.02–4.00 (m, 1H), 3.89–3.85 (m, 1H), 3.50–3.49 (m, 1H), 3.43–3.42 (m, 2H), 3.35 (s, 1H), 3.20–3.19 (m, 1H), 2.77 (s, 1H), 1.96–1.94 (m, 1H), 1.88–1.86 (m, 1H); ^{13}C NMR (151 MHz) δ 162.5 (2), 148.4, 140.1 (2), 133.7, 123.8 (3), 116.8, 107.5, 58.9, 56.4, 56.2, 48.4, 32.2, 22.6, 21.4. HRMS: calcd for $C_{18}H_{20}N_3O_3$·HCl [M-HCl + H]$^+$ 326.1499, found: 326.1489.

*4.1.8.9. 12N-4′-Methoxycarbonylbenzylcytisine hydrochloride (**5i**)*. The title compound was prepared from cytisine and methyl 4-bromomethylbenzoate in the same manner as described above. Yield: 69%; white solid; mp: 215–217 °C. ^{1}H NMR (600 MHz) δ 10.12 (br, 1H), 8.00 (d, J = 7.2 Hz, 2H), 7.73 (s, 2H), 7.40 (dd, J = 8.4, 7.2 Hz, 1H), 6.38 (d, J = 8.4 Hz, 1H), 6.23 (d, J = 6.6 Hz, 1H), 4.52–4.31 (m, 2H), 3.98–3.96 (m, 1H), 3.87 (s, 3H), 3.84–3.81 (m, 1H), 3.53–3.15 (m, 5H), 2.76 (s, 1H), 1.94–1.91 (m, 1H), 1.87–1.84 (m, 1H); ^{13}C NMR (151 MHz) δ 166.3, 162.8, 139.9 (2), 132.8, 131.1, 129.8 (4), 117.4, 106.7, 59.8, 56.7, 52.8 (2), 48.4, 32.4, 26.3, 23.0. HRMS: calcd for $C_{20}H_{23}N_2O_3$·HCl [M-HCl + H]$^+$ 339.1703, found: 339.1693.

*4.1.9. Synthesis of 12N-4′-carboxylbenzylcytisine sodium (**5j**)*

Compound **5i** (2 mmol) was dissolved in 20% NaOH (15 mL) and heated to reflux for 3 h. Then the pH of reaction solution was adjusted to 7–8 by hydrochloric acid. The reaction solvent was removed under reduced pressure. Then the residue was dissolved with MeOH and filtered to remove the inorganic salts. The solution was concentrated to obtain crude targeted compound, which was further separated by flash column chromatography on silica gel to afford purified title compounds. Yield: 76%; white solid; mp: 190–192 °C. ^{1}H NMR (600 MHz) δ 7.72 (d, J = 3.0 Hz, 2H), 7.39–7.31 (m, 1H), 6.89 (d, J = 6.6 Hz, 2H), 6.27 (d, J = 8.4 Hz, 1H), 6.02 (d, J = 6.6 Hz, 1H), 3.88–3.85 (m, 1H), 3.72–3.68 (m, 1H), 3.49–3.46 (m, 1H), 3.38–3.36 (m, 1H), 2.99 (s, 1H), 2.89–2.88 (m, 1H), 2.75–2.73 (m, 1H), 2.39–2.21 (m, 3H), 1.84–1.82 (m, 1H), 1.71–1.69 (m, 1H); ^{13}C NMR (151 MHz) δ 162.7, 152.5, 139.8, 139.2 (2), 129.4, 127.3 (4), 115.7, 104.3, 61.4, 60.1, 60.0, 50.1, 35.0, 27.9, 25.7. HRMS: calcd for $C_{19}H_{19}N_2NaO_3$ $[M + Na]^+$ 347.1366, found: 347.1360.

*4.1.10. Synthesis of 12N-1′,2′-phenylenedicytisine (**5k**)*

To a solution of cytisine (5 mmol) in acetonitrile (60 mL), K_2CO_3 (5 mmol) and 1,2-bisbromomethylbenzene (2 mmol) were added and stirred at room temperature until the TLC analysis showed completion of the reaction, then filtered. The filtrate was evaporated, and the residue was dissolved with CH_2Cl_2, washed with water, brine, dried. It was then filtered and concentrated to give a residue, which was purified by flash column chromatography on silica gel with CH_2Cl_2/CH_3OH as the eluent and then acidified with 2 N HCl/Et_2O to give the title compounds. Yield: 40%; white solid; mp: 220–222 °C. ^{1}H NMR (600 MHz) δ 7.34 (t, J = 7.2 Hz, 2H), 7.09–7.02 (m, 2H), 6.94–6.87 (m, 2H), 6.23 (d, J = 9.0 Hz, 2H), 6.01 (d, J = 6.0 Hz, 2H), 3.66–3.50 (m, 4H), 3.33 (s, 2H), 3.21–3.19 (m, 2H), 2.92–2.90 (m, 4H), 2.31–2.29 (m, 4H), 2.07–1.95 (m, 4H), 1.78–1.76 (m, 2H), 1.65–1.63 (m, 2H); ^{13}C NMR (151 MHz) δ 162.6 (2), 152.4 (2), 139.1 (2), 137.5 (2), 130.6 (2), 127.1 (2), 115.8 (2), 104.4 (2), 60.7 (2), 59.8 (2), 59.6 (2), 50.1 (2), 35.0 (2), 27.6 (2), 25.6 (2). HRMS: calcd for $C_{30}H_{35}N_4O_2$ $[M+H]^+$ 483.2754, found: 483.2743.

4.2. Biology assay

4.2.1. Cell culture and screening of compounds

The LX2 cell lines were transfected with COL1A1 promotor luciferase plasmid pGL4.17-COL1A1P using lipofactamine2000 followed the standard protocol (Invitrogen) for 24 h. Cells were laid on 96-well plate, cultured in Dulbecco's Modified Eagle's medium (DMEM), containing 10% fetal bovine serum (FBS) in a 5% CO_2 atmosphere at 37 °C. Moreover, serum-free culture was required until the cells at 90–95% confluence. After 24 h, cells were then treated simultaneously with TGFβ1 and a tested compounds (80 μM or 40 μM) for 24 h. The COL1A1 promotor activity was determined using the Bright-Glo luciferase assay system [14].

4.2.2. Cell survival assay

The cell survival was evaluated by MTT assay. HepG2 cells were seeded at density of 6 x10^3 cells/well in 96-well plate. Cells were treated with various concentrations of tested compounds until the cells at 50% confluence. After 24 h of incubation, 20 μL of the MTT (5 mg/mL) solution was added into each plate and incubated for 4 h at 37 °C, 5% CO_2. Subsequently, the culture supernatant was replaced with 150 μL DMSO to dissolve the formazan crystal. The absorbance at 570 nm was measured using a microplate reader.

4.2.3. RT-qPCR assay

LX-2 cells were seeded in 6-well plate, cultured in DMEM, containing 10% fetal bovine serum (FBS) in a 5% CO_2 atmosphere at 37 °C. And serum-free culture was required until the cells at 90–95% confluence. After 24 h, cells were treated with TGFβ1 (2 ng/mL) and tested derivatives (80 μM) for 24 h. Total RNA from the LX-2 cells was extracted using Trizol reagent, purified by NucleoSpin RNA Clean-up. Reverse transcription was performed with Transcriptor first strand cDNA synthesis kit. The cDNA was then analysis by ABI 7500 Fast RT-PCR System using TaqMan probes of TGFβ1, COL1A1, α-SMA, and GAPDH (sequence reserved by ABI) and FastStart Universal Probe master mix (Roche).

4.2.4. Western blot

LX-2 cells were cultured as described above. Briefly, cells were washed with phosphate-buffered saline (PBS) and were lysed in radioimmunoprecipitation assay (RIPA) lysis for 30 min in 4 °C; the supernatant was collected after centrifugation at 12,000 g, 4 °C for 15 min. Equal amounts of protein were quantified with Bradford assay, separated by SDS-PAGE and transferred to polyvinylidene difluoride membrane. The membranes were blocked for one hour at room temperature in PBST containing 5% milk and probed with specific first antibodies overnight at room temperature. Membrane was washed 3 times by PBST, followed by horseradish peroxidase-conjugated secondary antibodies and GAPDH. The proteins were visualized using chemiluminescence reagents.

4.3. Stability assay in whole blood

The fresh blood was collected from SD rat and pre-warmed in a water bath at 37 °C. 10 mM tested compounds or enalapril stock solutions were prepared in DMSO, and then diluted with 45% MeOH/H_2O to achieve 100 mM dosing solutions. Each dosing solution (2 mL) was

incubated with 98 mL of blank blood at 37 ℃ in water bath for 0, 0, 0.50, 1.0, 2.0, 4.0 and 8.0 h respectively. At the end of incubation, 100 mL water and 800 mL of stop solution (200 ng/mL tolbutamide plus 20 ng/mL buspirone in CH_3CN) were immediately added to precipitate protein and centrifuge at 4000 rpm for 20 min. An aliquot of supernatant (100 mL) was then extracted, mixed with 200 mL H_2O and then shook at 800 rpm for about 10 min before submitting to LC-MS/MS analysis. The experiment was repeated two times. 021

4.4. PK studies

Three male SD rats with weight of 190.0 ± 10.0 g were used in each study, which were purchased from SLAC Laboratory Animal Inc. (Shanghai, China). The experiment was performed in accordance with Guide for the Care and Use of Laboratory Animals, Eighth Edition. Each rat was administrated with compound **5f** or **5g** at 25 mg•kg^{-1} orally. Eight blood samples were collected at 0, 0.25, 0.50, 1.0, 2.0, 4.0, 6.0 and 8.0 h and were immediately centrifuged to separate the plasma fractions respectively. The separated plasma samples were stored at −20 ℃ for analysis. Concentration-versus-time profile was obtained for each analyze, and standard noncompartmental analysis was performed on the data using WinNonlin software, version 5.3, to recover the AUC and other non-compartmental parameters.

4.5. Acute toxicity

Female Kunming mice with weight of 20.0 ± 1.0 g were obtained from the Institute of Laboratory Animal Science (Beijing, China). The experiment was performed in accordance with the guidelines established by the National Institutes of Health for the care and use of laboratory animals. The mice were fed with regular rodent chow and housed in an air conditioned room. The mice were randomly divided into different groups with 6 mice each. Each compound was given orally in a single-dosing experiment at 0, 125, 250 or 500 mg•kg^{-1} (ddH_2O as control), respectively. The mice were closely monitored for 7 days. Body weight, behavior change and survival were monitored.

Acknowledgements

This work was supported by the National Natural Science Foundation of China (81621064 and 81673497) and CAMS initiative for innovative medicine (2017-12 M-3-012).

Declaration of Competing Interest

The authors declare no conflict of interest.

Appendix A. Supplementary material

Supplementary data to this article can be found online at https://doi.org/10.1016/j.bioorg.2019.103032.

References

[1] L. Campana, J.P. Iredale, Regression of liver fibrosis, Semin. Liver Dis. 37 (2017) 1–10.
[2] R.G. Romanelli, C. Stasi, Recent advancements in diagnosis and therapy of liver cirrhosis, Curr. Drug Targets 17 (2016) 1804–1817.
[3] E. Hashimto, M. Taniai, K. Tokushige, Characteristics and diagnosis of NAFLD/NASH, J. Gastroenterol. Hepatol. 28 (Suppl 4) (2013) 64–70.
[4] M.E. Zoubek, C. Trautwein, P. Strnad, Reversal of liver fibrosis: from fiction to reality, Best Pract. Res. Clin. Gastroenterol. 31 (2017) 129–141.
[5] C.Y. Zhang, W.G. Yuan, P. He, J.H. Lei, C.X. Wang, Liver fibrosis and hepatic stellate cells: etiology, pathological hallmarks and therapeutic targets, World J. Gastroenterol. 22 (2016) 10512–10522.
[6] H.M. Atta, Reversibility and heritability of liver fibrosis: Implications for research and therapy, World J. Gastroenterol. 21 (2015) 5138–5148.
[7] M. Sun, T. Kisseleva, Reversibility of liver fibrosis, Clin. Res. Hepatol. Gastroenterol. 39 (Suppl 1) (2015) S60–S63.
[8] R. Bataller, D.A. Brenner, Liver fibrosis, J. Clin. Invest. 115 (2005) 209–218.
[9] S.L. Friedman, Hepatic stellate cells: protean, multifunctional, and enigmatic cells of the liver, Physiol. Rev. 88 (2008) 125–172.
[10] J.P. Carson, G.A. Ramm, M.W. Robinson, D.P. McManus, G.N. Gobert, Schistosome-Induced Fibrotic Disease: The Role of Hepatic Stellate Cells, Trends Parasitol. 34 (2018) 524–540.
[11] K. Ikejima, K. Okumura, K. Kon, Y. Takei, N. Sato, Role of adipocytokines in hepatic fibrogenesis, J. Gastroenterol. Hepatol. 22 (Suppl 1) (2007) S87–S92.
[12] V. Krizhanovsky, M. Yon, R.A. Dickins, S. Hearn, J. Simon, C. Miething, H. Yee, L. Zender, S.W. Lowe, Senescence of activated stellate cells limits liver fibrosis, Cell 134 (2008) 657–667.
[13] S.S. Zhao, J.X. Wang, Y.C. Wang, R.G. Shao, H.W. He, Establishment and application of a high-throughput drug screening model based on COL1A1 promoter for anti-liver fibrosis, Yao Xue Xue Bao 50 (2015) 169–173.
[14] T. Niu, W. Niu, Y. Bao, T. Liu, D. Song, Y. Li, H. He, Discovery of matrinic thiadiazole derivatives as a novel family of anti-liver fibrosis agents via repression of the TGFβ/Smad pathway, Molecules 23 (2018) 1644.
[15] M. Ge, H. Liu, Y. Zhang, N. Li, S. Zhao, W. Zhao, Y. Zhen, J. Yu, H. He, R. Shao, The anti-hepatic fibrosis effects of dihydrotanshinone I are mediated by disrupting the yes-associated protein and transcriptional enhancer factor D2 complex and stimulating autophagy, Br. J. Pharmacol. 174 (2017) 1147–1160.
[16] J. Rouden, M.C. Lasne, J. Blanchet, J. Baudoux, (-)-Cytisine and derivatives: synthesis, reactivity, and applications, Chem. Rev. 114 (2014) 712–778.
[17] P. Tutka, W. Zatoński, Cytisine for the treatment of nicotine addiction: from a molecule to therapeutic efficacy, Pharmacol. Rep. 58 (2006) 777–798.
[18] D.K. Yu, C.X. Zhang, S.S. Zhao, S.H. Zhang, H. Zhang, S.Y. Cai, R.G. Shao, H.W. He, The anti-fibrotic effects of epigallocatechin-3-gallate in bile duct-ligated cholestatic rats and human hepatic stellate LX-2 cells are mediated by the PI3K/Akt/Smad pathway, Acta Pharmacol. Sin. 36 (2015) 473–482.
[19] A.W. Rachfal, D.R. Brigstock, Connective tissue growth factor (CTGF/CCN2) in hepatic fibrosis, Hepatol. Res. 26 (2003) 1–9.
[20] K.E. Lipson, C. Wong, Y. Teng, S. Spong, CTGF is a central mediator of tissue remodeling and fibrosis and its inhibition can reverse the process of fibrosis, Fibrogenesis Tissue Repair 5 (2012) 24–31.
[21] J.P. Iredale, Hepatic stellate cell behavior during resolution of liver injury, Semin. Liver Dis. 21 (2001) 427–436.
[22] T.Y. Fan, Y.X. Wang, S. Tang, X.X. Hu, Q.X. Zen, J. Pang, Y.S. Yang, X.F. You, D.Q. Song, Synthesis and antibacterial evaluation of 13-substituted cycloberberine derivatives as a novel class of anti-MRSA agents, Eur. J. Med. Chem. 157 (2018) 877–886.
[23] F. Xu, C. Liu, D. Zhou, L. Zhang, TGF-beta/SMAD pathway and its regulation in hepatic fibrosis, J. Histochem. Cytochem. 64 (2016) 157–167.
[24] K.A. El-Mihi, H.I. Kenawy, A. El-Karef, N.M. Elsherbiny, L.A. Eissa, Naringin attenuates thioacetamide-induced liver fibrosis in rats through modulation of the PI3K/Akt pathway, Life Sci. 15 (187) (2017) 50–57.
[25] K. Luo, Signaling Cross Talk between TGF-β/Smad and Other Signaling Pathways, Cold Spring Harb. Perspect. Biol. 9 (2017) a022137.